Modeling of Induction Machines Using a Voltage-Behind-Reactance Formulation

Liwei Wang, *Student Member, IEEE*, Juri Jatskevich, *Senior Member, IEEE*, and Steven D. Pekarek, *Member, IEEE*

***Abstract*—Over the past several years, there has been renewed interest in modeling electrical machines using phase (*abc*) variables. This paper considers modeling induction machines using phase variables in a voltage-behind-reactance (VBR) formulation. Specifically, three VBR models are proposed wherein the rotor electrical subsystem is modeled using flux linkages as state variables expressed in the *qd* reference frame. The stator electrical dynamics are represented in *abc* phase coordinates that enable direct interface of the machine model to an external network. Such a direct interface is advantageous when the machine is fed from a power electronic converter and/or when the modeling is carried out using circuit-based simulators. Computer studies of an induction machine demonstrate that the proposed VBR models achieve a 740% improvement in computational efficiency as compared with the traditional coupled-circuit phase-domain model.**

***Index Terms*—Coupled-circuit (CC) model, dynamic simulation, induction machine, *qd* model, voltage-behind-reactance (VBR) model.**

I. Introduction

THE MODELING of induction machines dates back to the early years of the 20th century [1]–[3]. Depending on the objective of studies and the required level of fidelity, the modeling approaches may be roughly divided into three categories: finite element (or difference) method [4]; equivalent magnetic circuit approach [5], [6]; and coupled electric circuit approach. This paper mainly considers the last approach, which leads to a relatively small number of equations. In particular, this paper focuses on the so-called general purpose models that are available in numerous simulation languages as built-in library components and by far the most commonly used by engineers and researchers in industry or academia (or at least attempted first, prior to constructing custom models). From this point of view, improving numerical accuracy and efficiency of such models even by a fraction may result in very significant savings of the engineering time worldwide.

Among the many methods developed, a key concept has been to transform physical (*abc*) variables of the machine into fictitious (*qd*) variables using rotating reference frames, e.g., stationary, rotor, or synchronous. The arbitrary reference frame (ARF) theory proposed in [7] generalized the *qd* modeling approach by showing that one can assign an appropriate reference speed ω to transform machine physical variables to a particular reference frame. The ARF provides a direct means of obtaining the machine equations in the aforementioned frames of reference.

The advantages of the *qd* induction machine models include the following: 1) the time-varying inductances between stator and rotor windings are eliminated; 2) the flux linkage equations are decoupled; 3) zero sequence quantities disappear for balanced operation and may be removed to reduce the number of state equations [8]; 4) the design of controls for machine drive systems can be conveniently developed in a reference frame in which variables become constant in the steady state [9]; and 5) the average-value modeling of machine-converter systems is simplified when expressing the machine in terms of *qd* variables [10]–[14].

Despite the many important advantages of using reference frame transformations when modeling systems that contain more than just a single machine, the *qd* model requires an interface with the external components or power electronics circuits. In many instances, the external components are modeled in *abc* physical variables (coordinates). Therefore, an interface is formed by the transformation (and inverse transformation), which poses an algebraic constraint.

For circuit- and/or nodal-analysis-based simulation languages, it is not easy to interface the *qd* equivalent circuits of the machine with the external network. Therefore, in simulation programs such as Electromagnetic Transients Program (EMTP) [15], prediction methods are often used [16], which reduce the simulation accuracy and efficiency by requiring small time steps and/or iterations. Interested reader may find more detailed discussions of the challenges associated with interfacing the *qd* model in [17]–[20], wherein the loss of stability and numerical accuracy have been documented.

In the state-variable languages, such as the widely used packages SimPowerSystem (SPS) [21] and Piece-wise Linear Electrical Circuit Simulation (PLECS) [22], the *qd* models are typically represented as voltage-controlled current sources [22], [23]. Therefore, such built-in *qd* models may not be directly interfaced with external circuits terminating with inductive branches, in which case, fictitious snubbers are often used to create the necessary voltages and enable the interface [21]–[24]. Discretizing the machine models separately from the main system-circuit is possible to avoid algebraic loops. For example, [21] permits discretizing the machine models using the Forward Euler method, while the external circuit may be

Manuscript received April 17, 2007; revised August 24, 2007. This work was supported in part by the Natural Sciences and Engineering Research Council (NSERC) of Canada under the Discovery Grant and in part by the Power Engineering Education and Research Grant from British Columbia Transmission Corporation and BC Hydro Inc. Paper no. TEC-00124-2007.

L. Wang and J. Jatskevich are with the Department of Electrical and Computer Engineering, University of British Columbia, Vancouver, BC V6T 1Z4, Canada (e-mail: liweiw@ece.ubc.ca; jurij@ece.ubc.ca).

S. D. Pekarek is with the Department of Electrical and Computer Engineering, Purdue University, West Lafayette, IN 47907 USA (e-mail: spekarek@purdue.edu).

Color versions of one or more of the figures in this paper are available online at http://ieeexplore.ieee.org.

Digital Object Identifier 10.1109/TEC.2008.918601

discretized using a fixed-step trapezoidal (Tustin) integration rule.

To simplify the machine model–network interface, several authors have suggested using the coupled-circuit (CC) phase-domain machine models [25]–[27], wherein the stator and rotor circuits are represented in *abc* phase coordinates. Using such an approach enables a direct connection between a machine and an external circuit. However, this approach comes at the cost of using a time-varying inductance matrix, which complicates the model and reduces its simulation efficiency. A hybrid approach that uses both *abc* phase variables for the stator circuit and *qd* stationary reference frame for the rotor circuit was proposed in [28]–[30]. Although the resulting machine inductance matrix does not depend on rotor position, these models use structural coupling between the stator and rotor and do not have a convenient equivalent-circuit representation. Therefore, it is a challenge to integrate these models with the external network systems using commonly available simulation languages.

A voltage-behind-reactance (VBR) model formulation was proposed for synchronous machines in [31] and [32] that also achieves the direct interface sought by the CC phase-domain model. As documented in [19], the VBR-based models are also very convenient for implementation in various nodal analysis- and circuit-based simulation packages and offer advantages in terms of numerical accuracy and efficiency.

This paper makes the following contributions in the area of modeling and numerical analysis of electrical machines:

1) We show that it is possible to extend the VBR formulation to a full-order induction machine model. In this formulation, the stator is expressed in *abc* direct-phase coordinates as three-phase dependent subtransient emf sources behind an *RL* circuit, and the rotor is expressed in transformed *qd* coordinates using fluxes as the independent variables.
2) It is also shown that the resulting VBR model can be expressed in several different forms, wherein, depending on the need, the *RL* circuit may be coupled or decoupled with an option of including the zero sequence wherever appropriate.
3) The proposed VBR model formulation enables a very straightforward and efficient interconnection of the stator *RL* circuit with the external circuit network, which is an advantage over all previously developed induction machine models.
4) The computer studies and eigenvalue analysis demonstrate that the proposed VBR machine model is computationally more efficient and accurate than the traditional CC model (that is typically used to achieve the direct interface) and/or or the classical *qd* model when it is interfaced using fictitious snubbers.

II. Coupled-Circuit Machine Model

To better understand the proposed advanced models, and for consistency purposes, CC model is reviewed here. Without the loss of generality, this paper assumes a three-phase, wye-connected, induction machine [9], whose cross-sectional view is shown in Fig. 1.

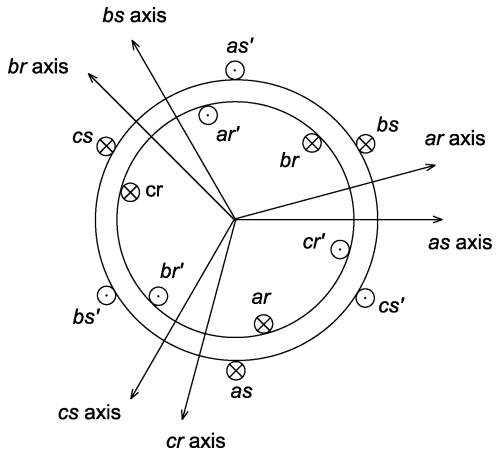

Fig. 1. Basic structure of an induction machine model.

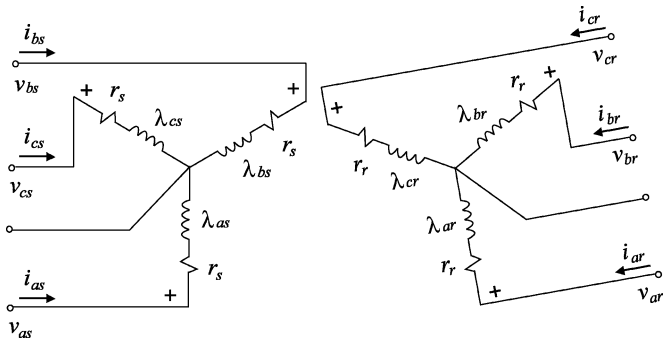

Fig. 2. CC model of induction machine.

The stator and rotor windings are assumed to be symmetric, sinusoidally distributed with resistance denoted by r_s and r_r, respectively. The positive direction of the magnetic axes corresponds to the direction of flux linkages induced by the positive phase currents. The induction machine may be represented in terms of coupled electric circuits, shown in Fig. 2. In this paper, motor convention is used, which assumes that positive stator and rotor currents flow into the machine when positive phase voltages are applied, as depicted in Fig. 2. For convenience, all rotor variables and parameters are referred to the stator side using an appropriate turns ratio.

The corresponding voltage equation may be expressed in matrix form as

$$\begin{bmatrix} \mathbf{v}_{abcs} \\ \mathbf{v}_{abcr} \end{bmatrix} = \begin{bmatrix} \mathbf{r}_s & \\ & \mathbf{r}_r \end{bmatrix} \begin{bmatrix} \mathbf{i}_{abcs} \\ \mathbf{i}_{abcr} \end{bmatrix} + p \begin{bmatrix} \lambda_{abcs} \\ \lambda_{abcr} \end{bmatrix} \tag{1}$$

where the stator and rotor diagonal resistance matrices are 3×3 and denoted by $\mathbf{r}_s$, $\mathbf{r}_r$, respectively. The operator p denotes d/dt. The corresponding flux linkage equation is

$$\begin{bmatrix} \boldsymbol{\lambda}_{abcs} \\ \boldsymbol{\lambda}_{abcr} \end{bmatrix} = \begin{bmatrix} \mathbf{L}_s & \mathbf{L}_{sr} \\ \mathbf{L}_{sr}^T & \mathbf{L}_r \end{bmatrix} \begin{bmatrix} \mathbf{i}_{abcs} \\ \mathbf{i}_{qdr} \end{bmatrix} \tag{2}$$

where the stator and rotor self-inductance matrices are $\mathbf{L}_s$ and $\mathbf{L}_r$, respectively, and are constant due to machine symmetry. The expressions for $\mathbf{L}_s$ and $\mathbf{L}_r$ can be found in [9] and are not included here due to space limitations. The mutual inductance

matrix has the following form:

$$\mathbf{L}_{sr} = L_{ms}\begin{bmatrix} \cos\theta_r & \cos\left(\theta_r + \frac{2\pi}{3}\right) & \cos\left(\theta_r - \frac{2\pi}{3}\right) \\ \cos\left(\theta_r - \frac{2\pi}{3}\right) & \cos\theta_r & \cos\left(\theta_r + \frac{2\pi}{3}\right) \\ \cos\left(\theta_r + \frac{2\pi}{3}\right) & \cos\left(\theta_r - \frac{2\pi}{3}\right) & \cos\theta_r \end{bmatrix}. \tag{3}$$

The developed electromagnetic torque may be expressed in direct physical machine variables as

$$T_e = \left(\frac{P}{2}\right)(\mathbf{i}_{abcs})^T \frac{\partial}{\partial\theta_r}[\mathbf{L}_{sr}]\,\mathbf{i}_{abcr}. \tag{4}$$

III. QD Machine Model in ARF

The CC induction machine model is often transformed into the *qd* arbitrary reference frame [9], where the flux linkages become decoupled. For convenient derivation of the VBR models, the *qd* model is included here in decoupled form. In particular, the voltage equations in the ARF are given as

$$v_{qs} = r_s i_{qs} + \omega\lambda_{ds} + p\lambda_{qs} \tag{5}$$

$$v_{ds} = r_s i_{ds} - \omega\lambda_{qs} + p\lambda_{ds} \tag{6}$$

$$v_{0s} = r_s i_{0s} + p\lambda_{0s} \tag{7}$$

$$v_{qr} = r_r i_{qr} + (\omega - \omega_r)\lambda_{dr} + p\lambda_{qr} \tag{8}$$

$$v_{dr} = r_r i_{dr} - (\omega - \omega_r)\lambda_{qr} + p\lambda_{dr} \tag{9}$$

$$v_{0r} = r_r i_{0r} + p\lambda_{0r}. \tag{10}$$

The flux linkage equations are expressed as

$$\lambda_{qs} = L_{ls} i_{qs} + \lambda_{mq} \tag{11}$$

$$\lambda_{ds} = L_{ls} i_{ds} + \lambda_{md} \tag{12}$$

$$\lambda_{0s} = L_{ls} i_{0s} \tag{13}$$

$$\lambda_{qr} = L_{lr} i_{qr} + \lambda_{mq} \tag{14}$$

$$\lambda_{dr} = L_{lr} i_{dr} + \lambda_{md} \tag{15}$$

$$\lambda_{0r} = L_{lr} i_{0r} \tag{16}$$

where magnetizing fluxes are defined as

$$\lambda_{mq} = L_m(i_{qs} + i_{qr}) \tag{17}$$

$$\lambda_{md} = L_m(i_{ds} + i_{dr}) \tag{18}$$

and

$$L_m = \frac{3}{2}L_{ms}. \tag{19}$$

The developed electromagnetic torque in terms of transformed *qd* variables is given as

$$T_e = \frac{3P}{4}(\lambda_{ds} i_{qs} - \lambda_{qs} i_{ds}). \tag{20}$$

IV. Voltage-Behind-Reactance Models in ARF

To derive the VBR model, it is necessary to formulate the stator voltage equation so that it appears similar to that of *RL*-branches, whereas the contribution due to the rotor subsystem is expressed in terms of dependent voltage sources. Since for an induction machine such model formulation is not unique, several models have been derived that may be of practical use, depending on the application.

A. Voltage-Behind-Reactance Model I

Derivation of the first model is performed by first solving (14) and (15) for currents and substituting the result into (17) and (18). The magnetizing fluxes are then expressed as

$$\lambda_{mq} = L''_m\left(i_{qs} + \frac{\lambda_{qr}}{L_{lr}}\right) \tag{21}$$

$$\lambda_{md} = L''_m\left(i_{ds} + \frac{\lambda_{dr}}{L_{lr}}\right) \tag{22}$$

where

$$L''_m = \left(\frac{1}{L_m} + \frac{1}{L_{lr}}\right)^{-1}. \tag{23}$$

Substituting (21) and (22) into (11) and (12), respectively, the stator flux linkage equations may be rewritten as

$$\lambda_{qs} = L'' i_{qs} + \lambda''_q \tag{24}$$

$$\lambda_{ds} = L'' i_{ds} + \lambda''_d \tag{25}$$

where the subtransient inductance is defined by

$$L'' = L_{ls} + L''_m. \tag{26}$$

The subtransient flux linkages are defined as

$$\lambda''_q = L''_m \frac{\lambda_{qr}}{L_{lr}} \tag{27}$$

$$\lambda''_d = L''_m \frac{\lambda_{dr}}{L_{lr}}. \tag{28}$$

Substituting (24) and (25) into (5) and (6), respectively, the stator voltage equations may be represented as

$$v_{qs} = r_s i_{qs} + \omega L'' i_{ds} + pL'' i_{qs} + \omega\lambda''_d + p\lambda''_q \tag{29}$$

$$v_{ds} = r_s i_{ds} - \omega L'' i_{qs} + pL'' i_{ds} - \omega\lambda''_q + p\lambda''_d. \tag{30}$$

The rotor currents are derived from (14) and (15) and are given by

$$i_{qr} = \frac{1}{L_{lr}}(\lambda_{qr} - \lambda_{mq}) \tag{31}$$

$$i_{dr} = \frac{1}{L_{lr}}(\lambda_{dr} - \lambda_{md}). \tag{32}$$

From (8), (9) and (31), (32), the rotor voltage equations may be rewritten as the following state equations

$$p\lambda_{qr} = -\frac{r_r}{L_{lr}}(\lambda_{qr} - \lambda_{mq}) - (\omega - \omega_r)\lambda_{dr} + v_{qr} \tag{33}$$

$$p\lambda_{dr} = -\frac{r_r}{L_{lr}}(\lambda_{dr} - \lambda_{md}) + (\omega - \omega_r)\lambda_{qr} + v_{dr}. \tag{34}$$

The terms $p\lambda_q''$ and $p\lambda_d''$ in the respective stator voltage equations (29) and (30) may be eliminated by taking the derivatives of (27) and (28) and substituting (33) and (34) into the resulting equations. After some algebraic manipulations, the stator voltage equations (29) and (30) may be rewritten in the following form

$$v_{qs} = r''i_{qs} + \omega L''i_{ds} + pL''i_{qs} + e_q'' \tag{35}$$

$$v_{ds} = r''i_{ds} - \omega L''i_{qs} + pL''i_{ds} + e_d'' \tag{36}$$

where

$$r'' = r_s + \frac{L_m''^2}{L_{lr}^2} r_r \tag{37}$$

and

$$e_q'' = \omega_r \lambda_d'' + \frac{L_m'' r_r}{L_{lr}^2}(\lambda_q'' - \lambda_{qr}) + \frac{L_m''}{L_{lr}} v_{qr} \tag{38}$$

$$e_d'' = -\omega_r \lambda_q'' + \frac{L_m'' r_r}{L_{lr}^2}(\lambda_d'' - \lambda_{dr}) + \frac{L_m''}{L_{lr}} v_{dr}. \tag{39}$$

The stator voltage equations (7), (35), and (36) may now be transformed back into the *abc* phase coordinates by applying inverse arbitrary reference transformation $(\mathbf{K}_s)^{-1}$. This final step gives the voltage equation in VBR form as

$$\mathbf{v}_{abcs} = \mathbf{r}_{abcs}''\mathbf{i}_{abcs} + \mathbf{L}_{abcs}''p\mathbf{i}_{abcs} + \mathbf{e}_{abcs}'' \tag{40}$$

where

$$\mathbf{e}_{abcs}'' = [\mathbf{K}_s]^{-1}[\, e_q'' \quad e_d'' \quad 0\,]^T. \tag{41}$$

Here, the resistance matrix is given by

$$\mathbf{r}_{abcs}'' = \begin{bmatrix} r_S & r_M & r_M \\ r_M & r_S & r_M \\ r_M & r_M & r_S \end{bmatrix} \tag{42}$$

where

$$r_S = r_s + r_a \tag{43}$$

$$r_M = -\frac{r_a}{2} \tag{44}$$

$$r_a = \frac{2}{3}\frac{L_m''^2}{L_{lr}^2} r_r. \tag{45}$$

The new inductance matrix is

$$\mathbf{L}_{abcs}'' = \begin{bmatrix} L_S & L_M & L_M \\ L_M & L_S & L_M \\ L_M & L_M & L_S \end{bmatrix} \tag{46}$$

where

$$L_S = L_{ls} + L_a \tag{47}$$

$$L_M = -\frac{L_a}{2} \tag{48}$$

$$L_a = \frac{2}{3} L_m''. \tag{49}$$

Note that, in (40), subtransient resistance matrix (42) and inductance matrix (46) are constant due to machine symmetry, and are independent of any reference frame. These are very desirable properties that make the VBR model more efficient than the CC model. Thus, equations (10), (33), (34), (38), (39), and (40) define the so-called VBR model formulation I (VBR-I).

Since in the VBR model formulation, there is no direct need to calculate the stator flux linkages λ_{qs} and λ_{ds}, the developed electromagnetic torque may be expressed using the magnetizing fluxes as [9]

$$T_e = \frac{3P}{4}(\lambda_{md} i_{qs} - \lambda_{mq} i_{ds}) \tag{50}$$

B. Voltage-Behind-Reactance Model II

The VBR-I contains a full resistance matrix (42), which may be difficult to implement in some simulation languages. As shown in [32], the model may be further simplified by using the diagonal stator resistance matrix $\mathbf{r}_s$ and moving the rotor resistance terms multiplied by stator currents i_{qs} and i_{ds} in (35) and (36), respectively, back into e_q'' and e_d''. This formulation constitutes the second VBR model II (VBR-II), which is expressed as

$$\mathbf{v}_{abcs} = \mathbf{r}_s\mathbf{i}_{abcs} + \mathbf{L}_{abcs}''p\mathbf{i}_{abcs} + \mathbf{v}_{abcs}''. \tag{51}$$

Here, other equations are the same as in VBR-I, except that the back emf $\mathbf{v}_{abcs}''$ is defined as

$$\mathbf{v}_{abcs}'' = [\mathbf{K}_s]^{-1}[\, v_q'' \quad v_d'' \quad 0\,]^T \tag{52}$$

where

$$v_q'' = \omega_r \lambda_d'' + \frac{L_m'' r_r}{L_{lr}^2}(\lambda_q'' - \lambda_{qr}) + \frac{L_m''}{L_{lr}} v_{qr} + \frac{L_m''^2 r_r}{L_{lr}^2} i_{qs} \tag{53}$$

$$v_d'' = -\omega_r \lambda_q'' + \frac{L_m'' r_r}{L_{lr}^2}(\lambda_d'' - \lambda_{dr}) + \frac{L_m''}{L_{lr}} v_{dr} + \frac{L_m''^2 r_r}{L_{lr}^2} i_{ds}. \tag{54}$$

Thus, the need for a mutual resistance matrix has been avoided [32].

C. Voltage-Behind-Reactance Model III

In both previous formulations, the stator inductive branches are coupled. A further simplification may be achieved if the stator inductance matrix (46) and resistance matrix (42) (in VBR-I) are made diagonal. The diagonalization may be carried out by first relating the stator current and zero-sequence current as [33]

$$i_{as} + i_{bs} + i_{cs} = 3i_{0s} \tag{55}$$

$$pi_{as} + pi_{bs} + pi_{cs} = 3pi_{0s}. \tag{56}$$

Here, we use (55) and (56) to reconsider the VBR-I formulation. The off-diagonal terms in the subtransient resistance and inductance matrices in (40) may be eliminated by expressing the stator currents associated with the off-diagonal entries in terms of the zero sequence current and the remaining phase (diagonal) current. After algebraic manipulations, (40) can be rewritten

as

$$\mathbf{v}_{abcs} = \begin{bmatrix} r_D & 0 & 0 \\ 0 & r_D & 0 \\ 0 & 0 & r_D \end{bmatrix} \mathbf{i}_{abcs} + \begin{bmatrix} L_D & 0 & 0 \\ 0 & L_D & 0 \\ 0 & 0 & L_D \end{bmatrix} p\mathbf{i}_{abcs} + \mathbf{e}''_{abcs} + \left(3r_M \begin{bmatrix} i_{0s} \\ i_{0s} \\ i_{0s} \end{bmatrix} + 3L_M \begin{bmatrix} pi_{0s} \\ pi_{0s} \\ pi_{0s} \end{bmatrix} \right) \tag{57}$$

where

$$r_D = r_S - r_M \tag{58}$$

and

$$L_D = L_S - L_M . \tag{59}$$

The voltage equation for the stator zero sequence is

$$v_{0s} = r_s i_{0s} + L_{ls} p i_{0s} \tag{60}$$

which gives the following state equation

$$pi_{0s} = \frac{1}{L_{ls}} \left(v_{0s} - r_s i_{0s} \right). \tag{61}$$

Substituting (61) into (57), the VBR model formulation III (VBR-III) has the following form

$$\mathbf{v}_{abcs} = \begin{bmatrix} r_D & 0 & 0 \\ 0 & r_D & 0 \\ 0 & 0 & r_D \end{bmatrix} \mathbf{i}_{abcs} + \begin{bmatrix} L_D & 0 & 0 \\ 0 & L_D & 0 \\ 0 & 0 & L_D \end{bmatrix} p\mathbf{i}_{abcs} + \mathbf{e}''_{abcs} + \left(3r_M - \frac{3L_M r_s}{L_{ls}} \right) \begin{bmatrix} i_{0s} \\ i_{0s} \\ i_{0s} \end{bmatrix} + \frac{3L_M}{L_{ls}} \begin{bmatrix} v_{0s} \\ v_{0s} \\ v_{0s} \end{bmatrix} \tag{62}$$

while other equations are the same as in VBR-I.

The same diagonalization procedure may be carried out with VBR-II to get its diagonal version, herein referred to as VBR-IV. However, it is not included here because the model structure of VBR-IV is very similar to VBR-III and no new features are added. As can be seen in (62), VBR-III has diagonal resistance and inductance matrices. A circuit-block diagram of the final VBR-III model is shown in Fig. 3. It should be noted that in this formulation, the *RL* circuit branches are decoupled from each other and have constant parameters. This feature provides a direct interface of the stator circuit with the external network, which makes it simpler to implement the induction machine in circuit-based simulation packages.

The VBR-III formulation depicted in Fig. 3 can be readily simplified if one assumes the wye-connected stator windings with a floating neutral, which is very common. In this case, the zero sequence variables simply disappear from (62) and Fig. 3, but the back emf $\mathbf{e}''_{abcs}$ remains the same as in VBR-I, (38), (39), and (41).

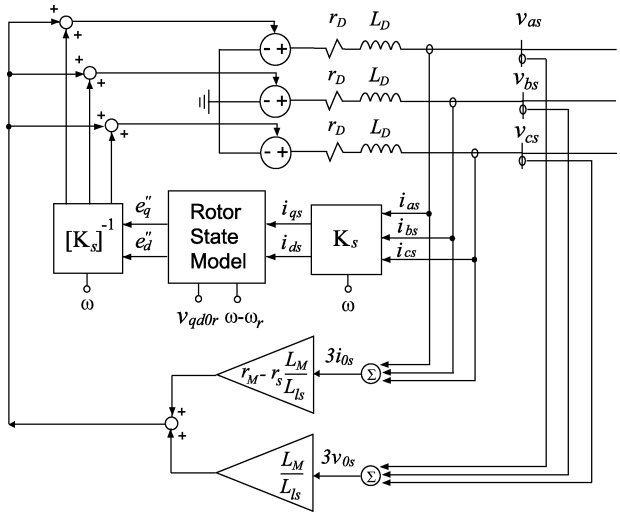

Fig. 3. Proposed VBR model formulation.

V. Computer Studies

All previously described models were implemented using MATLAB/Simulink [34]. Two types of *qd* model were used. The first one was a proper state-variable model implemented using standard/basic Simulink blocks. The resulting model/subsystem requires voltages as inputs and currents as outputs and has no circuit interface. The second *qd* machine model was the built-in SPS model [24]. SPS is a circuits-based simulation toolbox widely used for power- and power-electronic-systems transient simulations using Matlab/Simulink environment. The VBR models and the CC model were implemented using the circuit-based approach described in [35] and the toolbox [36]. In general, similar to a synchronous machine ([31], see Section V), the CC model could be implemented using either currents or the flux linkages as the state variables. However, if the stator circuit is to be interfaced with the external network where the currents are used as the independent variables, then machine currents must be considered as the state variables.

An induction machine with parameters summarized in Appendix B is considered here for simulating a no-load startup transient. Since the focus of this section is on component level, in the studies presented here, the machine is directly fed from an ideal balance three-phase voltage source. To evaluate the accuracy and efficiency of all models considered in this paper, the simulation studies were carried out using variable- as well as fixed-time-step integration methods.

A. Variable-Step Method

To make a fair comparison among the models, the same solver, ODE15s, was used for each model. To ensure smooth and accurate solution, the relative and absolute error tolerances were set to 10^{-4} and 10^{-6}, respectively. Also, the maximum and minimum time-step limits were set to 10^{-3} and 10^{-10} s, respectively, while the initial step was set to 10^{-5}s.

The transient responses produced by the *qd* models, three types of VBR models, and the CC model using the variable-step

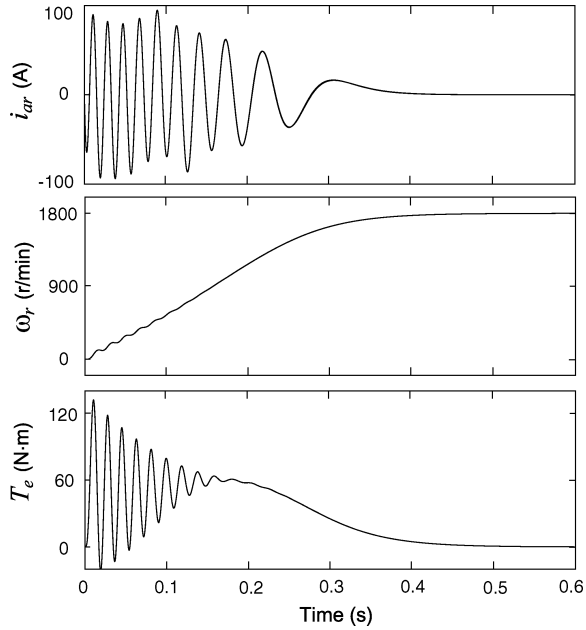

Fig. 4. Simulation results for six models using variable-step method.

TABLE I
SIMULATION EFFICIENCY COMPARISONS

Model	CPU Time, s	Num. of Steps	CPU Time per Step, μs
QD	0.062	744	83.3
CC	1.156	5283	218.8
SPS	0.313	1105	283.3
VBR-I	0.156	1036	150.6
VBR-II	0.157	1082	145.1
VBR-III	0.157	1075	146.0

integration method are depicted in Fig. 4. Due to space limitations, only the rotor current i_{ar}, the speed ω_r, and the electromagnetic torque T_e are shown. As can be seen in Fig. 4, all responses are visibly indistinguishable from each other. This result confirms that all models are consistent and equivalent, provided sufficiently small error tolerances and/or integration step size.

Assuming the same simulation accuracy for each model, the numerical efficiency of the models relative to each other may be evaluated by considering two factors: 1) the total number of integration steps taken to complete the study and 2) the computational load/cost per time step. The studies were run on a personal computer with an AMD 2200 processor using standard (not compiled, non-real-time) Simulink. The total CPU times, number of integration steps, and CPU times per step required to complete the study of Fig. 4 are summarized in Table I.

As can be seen in Table I, the bare-bones *qd* model, implemented in Simulink directly without circuit interface, has the fastest simulation speed (0.062 s) and the lowest computational cost requiring only 744 steps. The time-varying inductance matrix $\mathbf{L}(t)$ and the $p\mathbf{L}_{abc}$ term in the CC model (see Appendix A) leads to a significant increase in the CPU time per step (218.8 μs) as compared with the *qd* model (83.3 μs). In addition, the CC model requires significantly more time steps (5283) to achieve the same accuracy. The SPS machine model, when

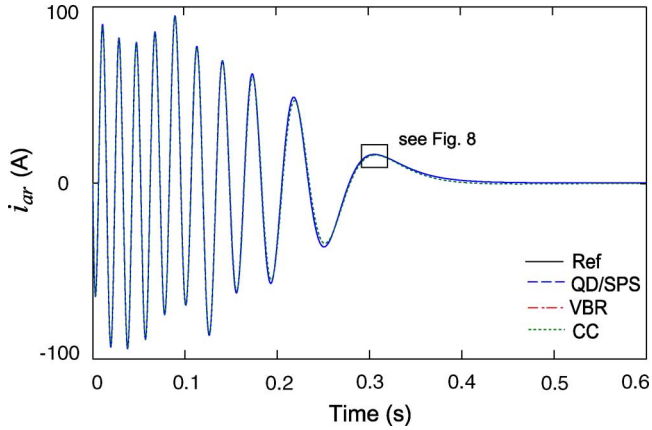

Fig. 5. Rotor current i_{ar} with time step of 1 ms.

fed by ideal voltage sources, preserves the advantage of the *qd* model and takes small number of time steps (1105), although some computational overhead exist in SPS that cause its model run slower (0.313 s) than the bare-bones Simulink *qd* model (0.062 s).

At the same time, all three VBR models performed very similarly to each other, which is expected since these models are algebraically equivalent, with only structural differences. The VBR models required more steps (1036–1082) and CPU time (0.157 s) than the bare-bones *qd* model, but generally performed by a factor of 2 faster than the SPS model (0.313 s). The proposed VBR models also demonstrated about 7.4 times improvement as compared with the CC model in terms of the overall CPU time required for the given study.

B. Fixed-Step Method

To further compare the numerical properties of the different models, the same case study is simulated with the fixed time-step integration method. To have a benchmark for comparing the simulation accuracy, a reference solution was obtained using the *qd* model with the fixed-step fourth-order Runge–Kutta integration method and a very small time step of 1 μs. The study was repeated for all considered models using the same fourth-order Runge–Kutta method, but with a much larger time step of 1 ms. The simulation results are shown in Figs. 5–7, where it can be seen that all models predict a similar response. However, it now becomes noticeable that the CC model (dotted line) is the farthest from the reference solution (solid line). A detailed view of the rotor current plot is shown in Fig. 8, wherein the plot is magnified to clearly show this difference.

Without the loss of generality, the rotor current trajectory is considered here to further quantify the numerical accuracy, since the other variables show a similar trend. The cumulative relative error between the reference solution $\tilde{i}_{ar}$ and a given numerical solution i_{ar}, as defined in terms of 2-norm [37], is evaluated as

$$\varepsilon(h) = \frac{\|\tilde{i}_{ar} - i_{ar}\|_2}{\|\tilde{i}_{ar}\|_2} \times 100\% \tag{63}$$

for different time steps h.

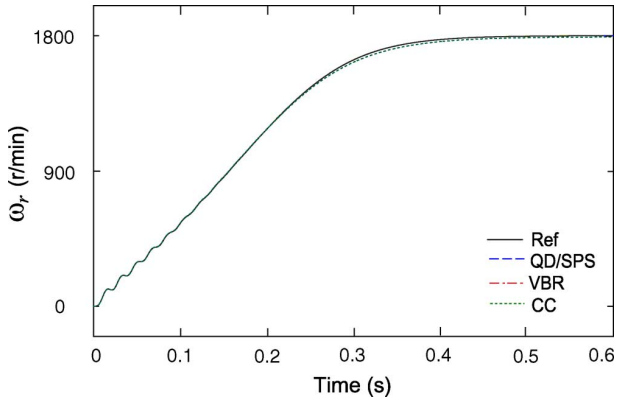

Fig. 6. Rotor rotating speed ω_r with time step of 1 ms.

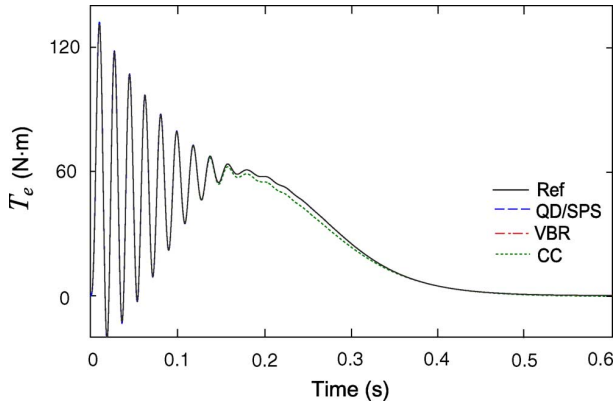

Fig. 7. Electromagnetic torque T_e with time step of 1 ms.

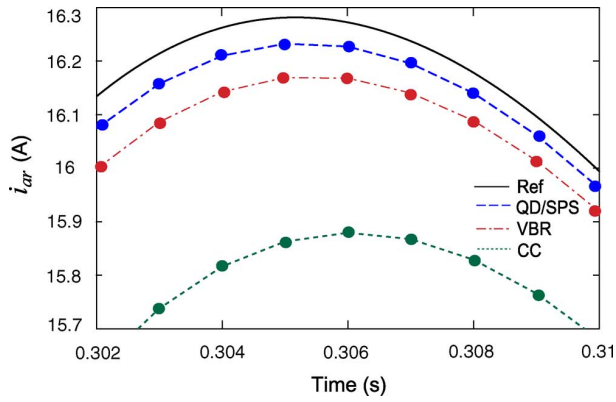

Fig. 8. Detailed view of rotor current i_{ar} with time step of 1 ms.

The simulation was run using time steps of 0.1, 0.5, and 1 ms. The calculated errors for the different models are shown in Fig. 9. As shown in Figs. 8 and 9, the bare-bones *qd* model and the SPS *qd* model produce exactly the same simulation results (shown in dashed line), and gave the smallest errors as compared with the other models. This is expected since the SPS uses the *qd* model internally, and the external circuit was just the ideal voltage sources. All of the VBR models (dash/dotted line) demonstrated identical results and accuracy, as all these models use similar state-space equations and differ only in the form of stator branches. The least accurate performance was demonstrated by the CC model (dotted line).

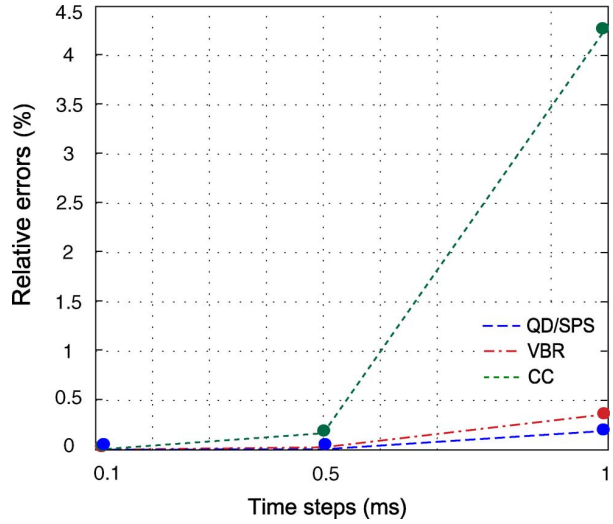

Fig. 9. Numerical error propagation of i_{ar}.

VI. Eigensystem Analysis

The *qd* models, the CC model, and the VBR models are all equivalent in the continuous time domain since these models are derived from each other without approximations. However, as demonstrated in Section V, the numerical properties of these models are quite different when the corresponding differential equations are discretized using an integration rule. In general, for nonlinear time-varying systems, the choice of state variables and/or the model structure may result in different eigenvalues of the system. The eigenvalues may influence the propagation of local errors, and therefore, affect the simulation accuracy when the differential equations are integrated numerically [38].

To gain some qualitative information and understanding of the numerical properties of the machine models described here, one may consider the state equations formed by the electrical circuit (see Fig. 2) of the machine [31]. In particular, if the rotor speed is assumed to be constant, the machine's nonlinear equations become linear, which allows one to express the corresponding system matrices. The resulting system matrices of various machine models are summarized in Appendix A, based on which the eigenvalues can be readily calculated. Alternatively, the respective models can be numerically linearized using a standard Matlab subroutine. Regardless of the approach, one should bear in mind that the eigenvalues of the induction machine model change quite significantly with speed [9, Ch. 8]. For comparison, the eigenvalues of all models were computed at an operating point close to steady state at no load (operating point corresponding to $t = 0.6$ s in the study shown in Fig. 4). The resulting eigenvalues are summarized in Table II.

In general, the negative real part of the eigenvalues is desirable for better damping, whereas positive eigenvalues tend to increase the local errors [39]. From this viewpoint, the *qd* model is well structured, since all of its eigenvalues are relatively far to the left side of the complex plane, as can be seen in Table II.

TABLE II
EIGENVALUES OF MACHINE MODELS

QD/SPS	CC	VBR-I, -II, -III
-19.52	1407	-0.016
-89.3 + j315.9	1406	-90.9 + j54.2
-89.3 - j315.9	0	-90.9 - j54.2
-218.1 + j60.4	-1723	-226.3 + j322.9
-218.1 - j60.4	-1724	-226.3 - j322.9
-217.5 / (N/A)	-217.5	-217.5
-408 / (N/A)	-408	-408

However, the CC model uses currents as state variables and has positive eigenvalues, which increases propagation of local errors, and therefore, reduces the simulation accuracy. A similar observation regarding the synchronous machine models has been made in [31].

An important observation can be made regarding the barebones *qd* model and the SPS *qd* model. In particular, the eigenvalues of these two models are identical, which also explains their identical simulation results in the previous studies. However, it should be noted that the SPS *qd* model ignores the stator and rotor zero sequence modes and that the two associated eigenvalues -217.5 and -408 are not present here.

Similar observation may be made for VBR models. Structurally, all three VBR models result in stator circuits (with constant stator inductances and resistances) that use currents as the independent variables, whereas the rotor subsystem uses flux linkages as the independent variables. Since these models are using the same set of state variables, their eigenvalues are identical, as shown in Table II. More importantly, the VBR models have negative eigenvalues, and therefore, their numerical properties are similar to those of the *qd* model, as was confirmed in Section V.

VII. DISCUSSION

The induction-machine models discussed in this paper may find their use depending on the modeling environment and application. For example, in differential-equation- or state-variable-based simulators (wherever there is no need to have a circuit interface), the machines may be considered as proper subsystems described by their corresponding equations. For these simulators, the *qd* model is perhaps the most accurate and simplest to use. However, for circuit-based simulation language, the machine stator windings must be made available for the interface with the external network. The CC phase-domain machine models are often used to fulfill this requirement; however, they are computationally more expensive and less accurate. The VBR models derived in this paper provide a good compromise among the models and offer very good structural as well numerical properties. Moreover, the final formulation VBR-III results in a decoupled (diagonal inductance and resistance matrices) time-invariant stator circuit, which allows a direct and simple interface of the stator branches with an external network.

To demonstrate the advantages of the VBR model over the *qd* model in terms of the model interface with the external network, it is sufficient to include small inductive impedance in the source, as shown in Fig. 10. Without the loss of generality, we

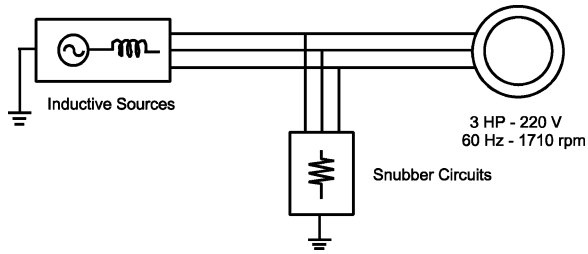

Fig. 10. Induction machine is fed from a voltage source with inductive impedance: artificial shunt resistors are used to interface the model.

conduct studies using the SPS and the proposed VBR model. The same machine as in Section V is used here, except that the voltage source has series inductance of 10^{-3} H in each phase. In the state-variable languages, the typical *qd* model is viewed and interfaced as a voltage-controlled current source (voltage input and current output). Therefore, the direct connection of machine terminals with inductive braches (or current sources) is not possible as it creates difficulties for forming the system's state space equations [21]–[24]. An approach that is often considered and suggested to the users for interfacing the machine models [22], [23] is to use an artificial shunt snubber circuit (very large resistors and/or small capacitors), which makes it possible to calculate the voltages at the interconnection point of the machine model and the external circuit, and therefore, completes the interface. In the studies presented here, to enable the SPS model interface, a shunt resistive branch was connected, as shown in Fig. 10. In general, the values of such artificial snubbers are chosen large enough as to minimize their effect on the simulation accuracy. However, when the VBR model is used, the stator *RL* branches are directly included into the external circuit network (see Fig. 3), and no artificial components are required.

The same startup transient study is performed for this case using the SPS *qd* model with snubber resistors of 10^3 Ω and the proposed VBR-III model. The same variable-step ODE solver and integration parameters (error tolerances and time-step limits) as in Section V-A are used here. The predicted responses are overlapped with the reference solution and shown in Figs. 11 and 12. Due to space limitation, only the rotor current i_{ar} is shown here. The reference solution are obtained using the barebone *qd* model with the fixed-step fourth-order Runge–Kutta integration method and a very small time step of 1 μs. In general, the transient trend is very similar to that shown in Section V (see Figs. 4 and 5), and the difference among the models is not noticed. This has been achieved by using relatively large values for the snubber resistors in the SPS model. However, the magnified plot of i_{ar} shown in Fig. 12 demonstrates that the SPS model actually converges to a different solution, which is shifted from the reference.

Another important observation that can be made based on Fig. 12 is that the SPS *qd* model uses significantly more time steps than the VBR model. To give the reader a better idea, the CPU times and the number of steps taken by the two models are summarized in Table III, where a very significant difference (an order of magnitude) can be seen.

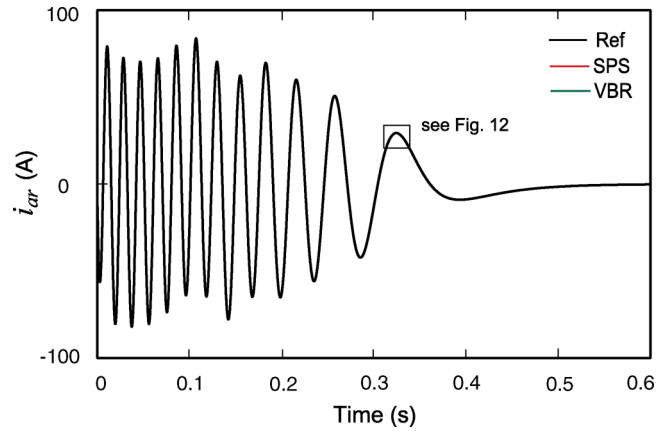

Fig. 11. Rotor current i_{ar} with variable-step method.

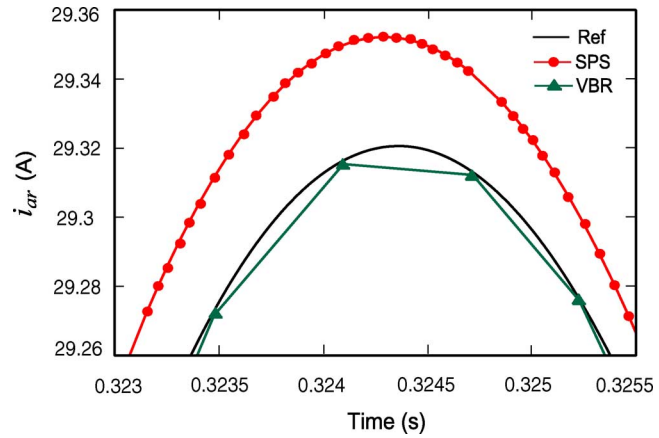

Fig. 12. Magnified portion of rotor current i_{ar} in Fig. 11.

TABLE III
SIMULATION EFFICIENCY COMPARISONS

Model	CPU Time, s	Num. of Steps	CPU Time per Step, μs
SPS	1.828	11504	158.9
VBR-III	0.156	1058	147.7

TABLE IV
EIGENVALUES OF MACHINE MODELS

SPS	VBR
-18.93	-0.016
-33.44 + j275.7	-79.5 + j33.6
-33.44 - j275.7	-79.5 - j33.6
-212.45 + j23.47	-175.9 + j343.5
-212.45 - j23.47	-175.9 - j343.5
-1.00e6	N/A
-1.25e6 + j76.27	N/A
-1.25e6 - j76.27	N/A

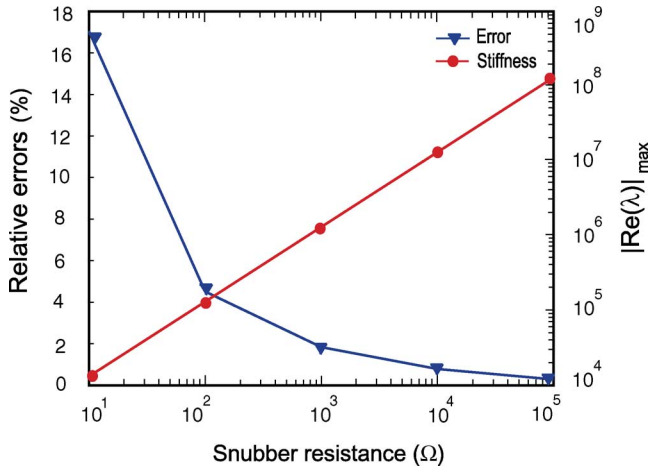

Fig. 13. Relative errors and stiffness of the SPS model for different snubber resistances.

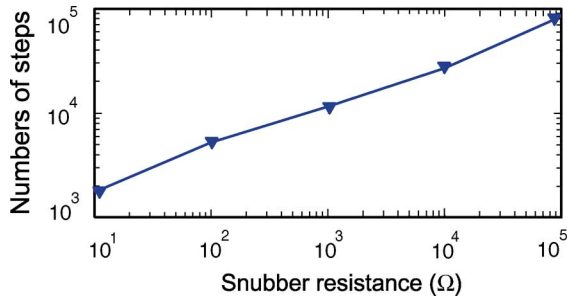

Fig. 14. Numbers of time steps required by the SPS model for different snubber resistances.

The presence of fictitious resistors also changes the network topology, as well as increases the total number of state variables due to the source inductance. Moreover, the resulting equations become very stiff, which can be noted by evaluating the eigenvalues summarized in Table IV, where it is shown that the SPS model now has three additional eigenvalues with very large magnitude on the order of 10^6. At the same time, for the VBR model, the source inductances do not increase the numbers of the eigenvalues and/or affect the stiffness. It may be noted that the VBR model in Table III does not include the eigenvalues corresponding to stator and rotor zero sequences, as it does in Table II. For discussion in this section and consistency with the SPS model, here the zero sequence was not included in the VBR model.

The affects of the snubber circuits on the simulation accuracy and efficiency may be further investigated by varying the values of resistors from 10 to 10^5 Ω. Without the loss of generality, here we again consider the relative errors for rotor current i_{ar}, which are calculated for the SPS model according to (63) and are plotted in Fig. 13. The magnitude of the largest negative eigenvalue is also plotted in Fig. 13 for the same range of snubber resistance. As can be seen here that it is possible to use very large resistors and achieve a high accuracy of such interface bring the errors below few percent. However, such improvement in accuracy comes at a price of making the system very stiff numerically.

The result of increasing numerical stiffness is that the ODE solver requires smaller and smaller time steps to satisfy the absolute and relative tolerances, which slows down the overall simulation. To give the reader a better idea, the number of time steps taken by the SPS model to complete the same transient study for the same range of snubber resistors is summarized in Fig. 14. As can be seen in Figs. 13 and 14, to achieve the solution within 1% of the reference solution, the SPS model requires the subbers of 10^5 Ω, which makes the system very stiff and bring

the number of time steps to the range of 10^5. At the same time, as evident from Fig. 9, the VBR model can achieve an even better accuracy with time steps as large as 1 ms requiring 600 steps total.

VIII. Conclusion

This paper presents a VBR induction machine model that can be of great benefit in applications where a direct interface of the stator phase branches with an external network circuit is required. Traditionally, in such applications, the CC phase-domain models are used, which results in significant increase in computational cost due to time-varying inductances. A method of interfacing the *qd* machine models with external inductive circuits in state-variable languages often requires artificial snubbers that also increase computational burden. However, the proposed VBR model, in addition to achieving the required direct interface of the stator circuit, also provides an improved numerical accuracy with greatly reduced computational overhead.

Appendix A

The system state matrices of the *qd* model with flux linkages as state variables are represented as

$$\mathbf{A}_{qd} = -\left(\mathbf{R}\mathbf{L}_{qd0}^{-1} + \mathbf{W}\right) \tag{A1}$$

where

$$\mathbf{R} = \mathrm{diag}[r_s, r_s, r_s, r_r, r_r, r_r] \tag{A2}$$

$$\mathbf{L}_{qd0} = \begin{bmatrix} L_{ls}+L_m & 0 & 0 & L_m & 0 & 0 \\ 0 & L_{ls}+L_m & 0 & 0 & L_m & 0 \\ 0 & 0 & L_{ls} & 0 & 0 & 0 \\ L_m & 0 & 0 & L_{lr}+L_m & 0 & 0 \\ 0 & L_m & 0 & 0 & L_{lr}+L_m & 0 \\ 0 & 0 & 0 & 0 & 0 & L_{lr} \end{bmatrix} \tag{A3}$$

$$\mathbf{W} = \begin{bmatrix} 0 & \omega & 0 & 0 & 0 & 0 \\ -\omega & 0 & 0 & 0 & 0 & 0 \\ 0 & 0 & 0 & 0 & 0 & 0 \\ 0 & 0 & 0 & 0 & \omega-\omega_r & 0 \\ 0 & 0 & 0 & -(\omega-\omega_r) & 0 & 0 \\ 0 & 0 & 0 & 0 & 0 & 0 \end{bmatrix}. \tag{A4}$$

The system state matrix of the CC model with currents as state variables may be expressed as

$$\mathbf{A}_{cc} = -\mathbf{L}_{abc}^{-1}\left(\mathbf{R} + p\mathbf{L}_{abc}\right) \tag{A5}$$

where

$$\mathbf{L}_{abc} = \begin{bmatrix} \mathbf{L}_s & \mathbf{L}_{sr} \\ \mathbf{L}_{sr}^T & \mathbf{L}_r \end{bmatrix}. \tag{A6}$$

For the VBR models, the state matrix is

$$\mathbf{A}_{vbr} = \begin{bmatrix} -\mathbf{L}''^{-1}_{abcs}\mathbf{r}''_{abcs} & -\mathbf{L}''^{-1}_{abcs}\mathbf{M}_1 \\ \mathbf{B}_2 & \mathbf{B}_1 \end{bmatrix} \tag{A7}$$

where

$$\mathbf{M}_1 = \mathbf{K}_s^{-1}\begin{bmatrix} \frac{L''_m r_r}{L_{lr}^2}\left(\frac{L''_m}{L_{lr}}-1\right) & \frac{\omega_r L''_m}{L_{lr}} & 0 \\ -\frac{\omega_r L''_m}{L_{lr}} & \frac{L''_m r_r}{L_{lr}^2}\left(\frac{L''_m}{L_{lr}}-1\right) & 0 \\ 0 & 0 & 0 \end{bmatrix} \tag{A8}$$

$$\mathbf{M}_2 = \begin{bmatrix} \frac{L''_m}{L_{lr}} & 0 & 0 \\ 0 & \frac{L''_m}{L_{lr}} & 0 \\ 0 & 0 & 0 \end{bmatrix} \tag{A9}$$

$$\mathbf{B}_1 = \begin{bmatrix} \frac{r_r}{L_{lr}}\left(\frac{L''_m}{L_{lr}}-1\right) & -(\omega-\omega_r) & 0 \\ \omega-\omega_r & \frac{r_r}{L_{lr}}\left(\frac{L''_m}{L_{lr}}-1\right) & 0 \\ 0 & 0 & -\frac{r_r}{L_{lr}} \end{bmatrix} \tag{A10}$$

$$\mathbf{B}_2 = \begin{bmatrix} \frac{r_r L''_m}{L_{lr}} & 0 & 0 \\ 0 & \frac{r_r L''_m}{L_{lr}} & 0 \\ 0 & 0 & 0 \end{bmatrix}\mathbf{K}_s. \tag{A11}$$

Appendix B

Induction machine parameters [9]: 3 hp, 220 V, 1710 r/min, 4 poles, 60 Hz, $r_s = 0.435\ \Omega$, $X_{ls} = 0.754\ \Omega$, $X_m = 26.13\ \Omega$, $r_r = 0.816\ \Omega$, $X_{lr} = 0.754\ \Omega$, $J = 0.089\ \mathrm{kgm}^2$.

Acknowledgment

The authors would like to thank their UBC and Purdue colleagues, as well as the reviewers and editor of this paper, for insightful and inspiring discussions contributing to this manuscript.

References

[1] H. C. Stanley, "An analysis of the induction motor," *AIEE Trans.*, vol. 57, pp. 751–755, 1938.
[2] D. S. Brereton, D. G. Lewis, and C. G. Young, "Representation of induction motor loads during power system stability studies," *AIEE Trans.*, vol. 76, pp. 451–461, Aug. 1957.
[3] G. Kron, *Equivalent Circuit of Electric Machinery*. New York: Wiley, 1951.
[4] S. J. Salon, *Finite Element Analysis of Electrical Machines*. Norwell, MA: Kluwer, 1995.
[5] G. R. Slemon, "An equivalent circuit approach to analysis of synchronous machines with saliency and saturation," *IEEE Trans. Energy Convers.*, vol. 5, no. 3, pp. 538–545, Sep. 1990.
[6] Y. Xiao, G. R. Slemon, and M. R. Iravani, "Implementation of an equivalent circuit approach to the analysis of synchronous machines," *IEEE Trans. Energy Convers.*, vol. 9, no. 4, pp. 717–723, Dec. 1994.
[7] P. C. Krause and C. H. Thomas, "Simulation of symmetrical induction machinery," *IEEE Trans. Power App. Syst.*, vol. 84, pp. 1038–1053, Nov. 1965.

[8] P. Kundur, *Power System Stability and Control*. New York: McGraw-Hill, 1994, Ch. 3.
[9] P. C. Krause, O. Wasynczuk, and S. D. Sudhoff, *Analysis of Electric Machinery and Drive Systems*, 2nd ed. Piscataway, NJ: IEEE Press, 2002.
[10] S. D. Sudhoff and O. Wasynczuk, "Analysis and average-value modeling of line-commutated converter-synchronous machine systems," *IEEE Trans. Energy Convers.*, vol. 8, no. 1, pp. 92–99, Mar. 1993.
[11] S. D. Sudhoff, K. A. Corzine, H. J. Hegner, and D. E. Delisle, "Transient and dynamic average-value modeling of synchronous machine fed load-commutated converters," *IEEE Trans. Energy Convers.*, vol. 11, no. 3, pp. 508–514, Sep. 1996.
[12] B. T. Kuhn, S. D. Sudhoff, and C. A. Whitcomb, "Performance characteristics and average-value modeling of auxiliary resonant commutated pole converter based induction motor drives," *IEEE Trans. Energy Convers.*, vol. 14, no. 3, pp. 493–499, Sep. 1999.
[13] J. Jatskevich, S. D. Pekarek, and A. Davoudi, "Parametric average-value model of synchronous machine-rectifier systems," *IEEE Trans. Energy Convers.*, vol. 21, no. 1, pp. 9–18, Mar. 2006.
[14] J. Jatskevich, S. D. Pekarek, and A. Davoudi, "Fast procedure for constructing an accurate dynamic average-value model of synchronous machine-rectifier systems," *IEEE Trans. Energy Convers.*, vol. 21, no. 2, pp. 435–441, Jun. 2006.
[15] H. W. Dommel, *EMTP Theory Book*. Vancouver, BC, Canada: Micro-Tran Power System Analysis Corporation, May 1992, Ch. 8.
[16] V. Brandwajn, "Synchronous generator models for the analysis of electromagnetic transients," Ph.D. thesis, Univ. British Columbia, Vancouver, BC, Canada, 1977.
[17] X. Cao, A. Kurita, H. Mitsuma, Y. Tada, and H. Okamoto, "Improvements of numerical stability of electromagnetic transient simulation by use of phase-domain synchronous machine models," *Electr. Eng. Jpn.*, vol. 128, no. 3, pp. 53–62, Apr. 1999.
[18] A. B. Dehkordi, A. M. Gole, and T. L. Maguire, "Permanent magnet synchronous machine model for real-time simulation," presented at the Interracial Conf. Power Syst. Transients (IPST'05), Montreal, Canada.
[19] L. Wang and J. Jatskevich, "A voltage-behind-reactance synchronous machine model for the EMTP-type solution," *IEEE Trans. Power Syst.*, vol. 21, no. 4, pp. 1539–1549, Nov. 2006.
[20] L. Wang, J. Jatskevich, and H. W. Dommel, "Re-examination of synchronous machine modeling techniques for electromagnetic transient simulations," *IEEE Trans. Power Syst.*, vol. 22, no. 3, pp. 516–527, Aug. 2007.
[21] SimPowerSystems 4–User Guide, The MathWorks, Inc., Natick, Massachusetts [Online]. Available at: www.mathworks.com, 2007.
[22] Piecewise Linear Electrical Circuit Simulation (PLECS) User Manual, Version. 1.5, Plexim GmbH [Online]. Available at: www.plexim.com, 2006.
[23] R. Champagne, L.-A. Dessaint, H. Fortin-Blanchette, and G. Sybille, "Analysis and validation of a real-time AC drive simulator," *IEEE Trans. Power Electron.*, vol. 19, no. 2, pp. 336–345, Mar. 2004.
[24] SimPowerSystems 4–Reference Manual, The MathWorks, Inc., Natick, Massachusetts [Online]. Available at: www.mathworks.com, 2007.
[25] J. R. Marti and T. O. Myers, "Phase-domain induction motor model for power system simulators," *IEEE Conf. Commun., Power, Comput.*, vol. 2, May 1995, pp. 276–282.
[26] J. R. Marti and K. W. Louie, "A phase-domain synchronous generator model including saturation effects," *IEEE Trans. Power Syst.*, vol. 12, no. 1, pp. 222–229, Feb. 1997.
[27] W. Gao, E. V. Solodovnik, and R. A. Dougal, "Symbolically aided model development for an induction machine in virtual test bed," *IEEE Trans. Energy Convers.*, vol. 19, no. 1, pp. 125–135, Mar. 2004.
[28] R. W. Y. Cheung, H. Jin, B. Wu, and J. D. Lavers, "A generalized computer-aided formulation for the dynamic and steady state analysis of induction machine inverter drive systems," *IEEE Trans. Energy Convers.*, vol. 5, no. 2, pp. 337–343, Jun. 1990.
[29] C. T. Liu and W. L. Chang, "A generalized technique for modeling switch-controlled induction machine circuits," *IEEE Trans. Energy Convers.*, vol. 7, no. 1, pp. 168–176, Mar. 1992.
[30] P. Pillay and V. Levin, "Mathematical models for induction machines," in *Proc. Rec. 1995 IEEE Ind. Appl. Conf., 30th IAS Annu. Meet.*, vol. 1, no. 8–12, Oct. 1995, pp. 606–616.
[31] S. D. Pekarek, O. Wasynczuk, and H. J. Hegner, "An efficient and accurate model for the simulation and analysis of synchronous machine/converter systems," *IEEE Trans. Energy Conv.*, vol. 13, no. 1, pp. 42–48, Mar. 1998.
[32] W. Zhu, S. D. Pekarek, J. Jatskevich, O. Wasynczuk, and D. Delisle, "A model-in-the-loop interface to emulate source dynamics in a zonal DC distribution system," *IEEE Trans. Power Electron.*, vol. 20, no. 2, pp. 438–445, Mar. 2005.
[33] R. R. Nucera, S. D. Sudhoff, and P. C. Krause, "Computation of steady-state performance of an electronically commutated motor," *IEEE Trans. Ind. Appl.*, vol. 25, no. 6, pp. 1110–1117, Nov./Dec. 1989.
[34] Simulink Dynamic System Simulation Software–Users Manual, MathWorks, Inc., Natick, Massachusetts, 2005.
[35] O. Wasynczuk and S. D. Sudhoff, "Automated state model generation algorithm for power circuits and systems," *IEEE Trans. Power Syst.*, vol. 11, no. 4, pp. 1951–1956, Nov. 1996.
[36] Automated State Model Generator (ASMG), Reference Manual, Version 2, PC Krause and Associates Inc. [Online]. Available at: www.pcka.com, 2002.
[37] W. Gautchi, *Numerical Analysis: An Introduction*. Boston, MA: Birkhauser, 1997.
[38] L. O. Chua and P-M Lin, *Computer Aided Analysis of Electronic Circuit: Algorithms and Computational Techniques*. Englewood Cliffs, NJ: Prentice-Hall, pp. 43–45, 1975.
[39] Uri Ascher and L. R. Petzold, *Computer Methods for Ordinary Differential Equations and Differential-Algebraic Equations*. Philadelphia, PA: SIAM, 1998, Ch. 2.

Liwei Wang (S'04) received the M.S. degree in electrical engineering from Tianjin University, Tianjin, China, in 2004. He is currently working toward the Ph.D. degree in electrical and computer engineering from the University of British Columbia, Vancouver, BC, Canada.

His current research interests include electrical machines, power, and power electronic systems simulation.

Juri Jatskevich (M'99–SM'07) received the M.S.E.E. and Ph.D. degrees in electrical engineering from Purdue University, West Lafayette, IN, in 1997 and 1999, respectively.

He was Post-Doctoral Research Associate and Research Scientist at Purdue University, as well as consulted for P C Krause and Associates, Inc. Since 2002, he has been a faculty member at the University of British Columbia, Vancouver, Canada, where he is now an Associate Professor of Electrical and Computer Engineering. His research interests include electrical machines, power electronic systems, average-value modeling and simulation.

Dr. Jatskevich is presently a Secretary of IEEE CAS Power Systems & Power Electronic Circuits Technical Committee, Editor of IEEE TRANSACTIONS ON ENERGY CONVERSION, and Editor of IEEE POWER ENGINEERING LETTERS. He is also chairing the IEEE Task Force on Dynamic Average Modeling, under the Working Group on Modelling and Analysis of System Transients Using Digital Programs.

Steven D. Pekarek (M'96) received the Ph.D. degree in electrical engineering from Purdue University, West Lafayette, IN, in 1996.

During 1997–2004, he was an Assistant (Associate) Professor of Electrical and Computer Engineering at the University of Missouri-Rolla (UMR). He is currently a Professor of Electrical and Computer Engineering at Purdue University and is a Co-Director of the Energy Systems Analysis Consortium. As a faculty member, he has been the Principal Investigator on several research programs, including projects for the Navy, Airforce, Ford Motor Corporation, Motorola, and Delphi Automotive Systems. His current research interests include power electronic-based architectures for finite inertia power and propulsion systems.

Prof. Pekarek is an active member of the IEEE Power Engineering Society, the Society of Automotive Engineers, the IEEE Power Electronics Society, and he was Chairman of the 2005 International Future Energy Challenge.